

Extended Object Tracking with Random Hypersurface Models

MARCUS BAUM
UWE D. HANEBECK
Karlsruhe Institute of Technology (KIT)

The random hypersurface model (RHM) is introduced for estimating a shape approximation of an extended object in addition to its kinematic state. An RHM represents the spatial extent by means of randomly scaled versions of the shape boundary. In doing so, the shape parameters and the measurements are related via a measurement equation that serves as the basis for a Gaussian state estimator. Specific estimators are derived for elliptic and star-convex shapes.

Manuscript received February 24, 2012; revised December 10, 2012; released for publication April 17, 2013.

IEEE Log No. T-AES/50/1/944778.

DOI. No. 10.1109/TAES.2013.120107.

Refereeing of this contribution was handled by W. Koch.

Authors' address: Intelligent Sensor-Actuator-Systems Laboratory (ISAS), Institute for Anthropomatics, Karlsruhe Institute of Technology (KIT), Germany. E-mail: (marcus.baum@kit.edu and uwe.hanebeck@ieee.org).

0018-9251/14/\$26.00 © 2014 IEEE

I. INTRODUCTION

In target tracking applications [1] where the resolution of the sensor device is higher than the spatial extent of a target object, the usual point object assumption is not justified as several different points, i.e., measurement sources, on the target object may be resolved (see Fig. 1). The resolved measurement sources typically vary from scan to scan and their locations depend on the shape of the object but also on further properties such as the surface or the target-to-sensor geometry.

In this article the basic idea is to approximate an extended object with a geometric shape such as an ellipse [2–4] as depicted in Fig. 1. The tracking problem then consists of estimating the shape parameters in addition to the kinematic parameters. The locations of the measurement sources are not explicitly estimated. Reasonably, the shape of the target should be described as detailed as possible. However, when the measurement noise is rather high and only a few measurements are available, it may only be possible to infer a coarse shape approximation such as a circle.

The unknown locations of the measurement sources are usually modeled with a probability distribution whose mass is concentrated on the extended object (a so-called spatial distribution) [2, 5]. In general, no closed-form solutions for the likelihood function resulting from a spatial distribution model exist, so that Monte-Carlo methods are frequently used for approximating the Bayesian filter solution [2, 5–10]. In case of an elliptic extent [3, 11–15], closed-form expressions can be derived with the help of random matrix theory. Spatial distributions have been embedded into the probability hypothesis density (PHD) filter for tracking multiple extended objects [16–20]. In [21, 22], it is proposed to drop all statistical assumptions on the measurement sources, which leads to a combined set-theoretic and stochastic estimator.

A. Contributions

The main contribution is a novel systematic approach for modeling the unknown location of a measurement source on a spatially extended object called random hypersurface model (RHM). The basic idea is to assume the measurement source to lie on a scaled version of the shape boundary, where the scaling factor is modeled as a random variable. In this manner it is possible to form a suitable measurement equation that serves as the basis for constructing a Gaussian state estimator. In order to illustrate the novel approach, specific RHMs and corresponding Gaussian estimators are developed for ellipses and free-form star-convex shapes. To the best of our knowledge, this is the first extended object tracking method for explicitly estimating a free-form star-convex shape approximation. Actually, with this method, it is possible to track a target whose shape is a priori unknown and estimated from scratch over time.

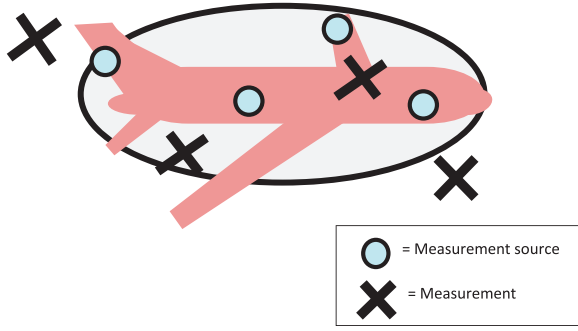


Fig. 1. Shape approximation of extended object with ellipse.

REMARK 1 This article is based on [4, 23–30].

The remainder of this article is structured as follows. In the following section the general probabilistic framework for extended object tracking is presented. The new target extent model called random hypersurface model is subsequently introduced in Section III. Based on these models, a formal Bayes filter for extended object tracking is described in Section IV. Then, particular implementations of RHM for ellipses (Section V) and star-convex shapes (Section VI) are developed. Both shape representations are evaluated by means of typical extended object tracking scenarios in Section VII. This article is concluded in Section VIII.

II. MODELING EXTENDED TARGETS

The state vector of the extended object at discrete time k is represented with a random vector¹ $\underline{x}_k = [\underline{m}_k^T, (\underline{x}_k^*)^T, \underline{p}_k^T]^T$ that consists of the target location \underline{m}_k , a shape parameter vector \underline{p}_k , and an optional vector \underline{x}_k^* for the kinematics, e.g., velocity. The shape parameter \underline{p}_k specifies a two-dimensional set that is denoted with $S(\underline{p}_k) \subset \mathcal{R}^2$. For example, a circular shape can be specified by its radius r_k , i.e., $p_k^{\text{ci}} = r_k$ and the corresponding shape is $S(p_k^{\text{ci}}) = \{\underline{z} \mid \underline{z} \in \mathcal{R}^2 \text{ and } \|\underline{z}\|_2 \leq r_k\}$.² Note that we focus on two-dimensional shapes. Nevertheless the concepts are also applicable to higher dimensional shapes in the same manner; see for example [31].

A. Measurement Model

At each time step k , a set of n_k two-dimensional point measurements $\{\hat{y}_{k,l}\}_{l=1}^{n_k}$ of the extended object is available. We assume the measurements to be mutually independent for given target state; hence, a measurement model for a single measurement is sufficient.

Extent Model: For a given state \underline{x}_k , the target extent model specifies a single measurement source $\underline{z}_{k,l} \in \underline{m}_k + S(\underline{p}_k)$ on the extended object (see Fig. 2).³ In the following

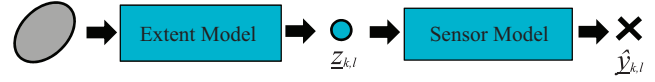


Fig. 2. Measurement model for single measurement.

Section III, we introduce the so-called RHM for the target extent.

Sensor Model: For a given measurement source $\underline{z}_{k,l}$, the sensor model specifies the measurement $\hat{y}_{k,l}$. We focus on Cartesian point measurements corrupted with additive Gaussian noise according to

$$\hat{y}_{k,l} = \underline{z}_{k,l} + \underline{v}_{k,l} \quad (1)$$

where the noise term $\underline{v}_{k,l}$ is zero-mean white Gaussian noise with covariance matrix $\sum_{k,l}^v$.

B. Dynamic Model

In contrast to a point target, the temporal evolution of both the shape and kinematic parameters has to be modeled for an extended object. In this article we focus on linear motion models according to

$$\underline{x}_{k+1} = \mathbf{A}_k \underline{x}_k + \underline{w}_k \quad (2)$$

where \mathbf{A}_k is the system matrix and \underline{w}_k is white Gaussian system noise.

III. RANDOM HYPERSURFACE MODELS

In this section a new target extent model called RHM is introduced, which describes the location of a single measurement source in a star-convex region.⁴

DEFINITION 1 (Star-Convexity). A set $S \subset \mathcal{R}^2$ is star-convex with respect to the origin iff $[0, 0]^T \in S$ and each line segment from $[0, 0]^T$ to any point in S is fully contained in S .

A. Motivation: Implicit Measurement Equation

The objective is to form an equation that relates the measurement source with the shape parameters. When the measurement source $\underline{z}_{k,l}$ lies on the boundary of the object, this is easy as the boundary is a closed curve (in general a hypersurface) that can be described by an implicit equation in the form $g(\underline{z}_{k,l}, \underline{p}_k) = 0$. However, the measurement sources may also lie in the interior of boundary. In order to cover the interior, the basic idea is to scale the object boundary as described in Fig. 3. As the corresponding scaling factor $s_{k,l} \in [0, 1]$ for a measurement source $\underline{z}_{k,l}$ is unknown, we model it as a random variable and treat it as an additional noise term. By this means we define the implicit relation

$$\tilde{g}(\underline{z}_{k,l}, \underline{P}_k, s_{k,l}) = 0 \quad (3)$$

¹In this article vectors are underlined, e.g., \underline{x} is a vector.

²ci in p_k^{ci} indicates that it parameterizes a circle.

³Set operations “+” and “.” meant element-wise.

⁴The concept of an RHM is much more general than presented here. The restriction to (two-dimensional) star-convex shapes is done for simplifying the following discussions.

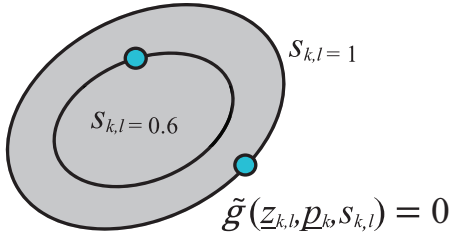


Fig. 3. RHM for ellipse.

which forms, together with (1), an implicit measurement equation (note that $\tilde{g}(\underline{z}_{k,l}, \underline{p}_k, 1) = g(\underline{z}_{k,l}, \underline{p}_k)$). In this sense modeling a two-dimensional region is reduced to modeling a curve by means of the scaling factor.

B. Definition

According to the above motivation, RHMs assume that the measurement source is an element of a scaled version of the shape boundary, where the scaling factor is characterized by a particular probability distribution, i.e., the scaling factor is modeled as a one-dimensional random variable.

DEFINITION 2 (Random Hypersurface Model). The measurement source $\underline{z}_{k,l} \in \underline{m}_k + S(\underline{p}_k)$ on an extended object with star-convex shape $S(\underline{p}_k) \subset \mathcal{R}^2$ and center $\underline{m}_k \in S(\underline{p}_k)$ is generated according to an RHM if

$$\underline{z}_{k,l} \in \underline{m}_k + s_{k,l} \cdot S(\underline{p}_k)$$

where $\bar{S}(\underline{p}_k)$ denotes the boundary of $S(\underline{p}_k)$ and $s_{k,l} \in [0, 1]$ is a one-dimensional random variable.

The restriction to star-convex shapes ensures that $S(\underline{p}_k) = \cup_{s \in [0,1]} \{s \cdot S(\underline{p}_k)\}$. In fact scaling the object boundary corresponds to a straight-line homotopy from the object center to the object boundary. Note that all scaling factors $s_{k,l}$ are mutually independent because measurements are assumed to be mutually independent.

Definition 2 does not specify where the measurement source $\underline{z}_{k,l}$ lies on the scaled boundary. In general it is possible to consider it as an unknown fixed parameter (functional model) or to assume it to be drawn from a probability distribution (structural model). These two models are also widely used in curve fitting [32]. For the structural model, an RHM becomes a spatial distribution model [2, 5].

REMARK 2 The implicit representation motivated in Section III-A is based on the functional model. Probabilistic information about the location of a measurement source on the boundary is not explicitly encoded in the implicit function.

The shape boundary can be written as

$$\bar{S}(\underline{p}_k) = \{\underline{z} | \underline{z} \in \mathcal{R}^2 \text{ and } g(\underline{z}, \underline{p}_k) = 0\} \quad (4)$$

and

$$s_{k,l} \cdot \bar{S}(\underline{p}_k) = \{\underline{z} | \underline{z} \in \mathcal{R}^2 \text{ and } \tilde{g}(\underline{z}, \underline{p}_k, s_{k,l}) = 0\} \quad (5)$$

is the scaled shape boundary.

C. Probability Distribution of the Scaling Factor

The probability distribution of the scaling factor depends on the distribution of the measurement sources on the extended object. The following theorem says how the scaling factor is distributed in case the measurement sources are uniformly distributed on the surface of a two-dimensional extended object.

THEOREM 1. *If the measurement source $z \in \mathcal{R}^2$ is uniformly distributed over the star-convex region $S \subset \mathcal{R}^2$ with center $[0, 0]^T$, the corresponding squared scaling factor is uniformly distributed on the interval $[0, 1]$.*

PROOF. The cumulative distribution function $F(s)$ of (s) turns out to be

$$F(s) = p(s \leq s) = p(\underline{z} \in s \cdot S) = \frac{\text{Area}(s \cdot S)}{\text{Area}(S)} = s^2 \quad (6)$$

for $s \in [0, 1]$. Additionally, $F(s) = 0$ for $s < 0$ and $F(s) = 1$ for $s > 1$. The cumulative distribution of $u := s^2$ given by $F(u) = p(s \leq \sqrt{u})$ is the cumulative distribution function of the uniform distribution on $[0, 1]$.

According to theorem 1 it is reasonable to choose a uniform distribution for the squared scaling factor.

D. General Procedure for Extended Object Tracking with RHMs

In order to derive a state estimator for an extended object based on an RHM, the following steps are to be performed.

- 1) A suitable shape and a shape parameterization have to be determined.
- 2) The implicit equation (3) has to be formed.
- 3) A state estimator has to be derived based on the implicit measurement equation defined by (3) and (1).

Based on the above steps, we will derive particular Gaussian estimators for ellipses and free-form star-convex shapes.

IV. FORMAL GAUSSIAN STATE ESTIMATOR FOR EXTENDED OBJECTS

In the following the notation of a formal (Gaussian) Bayes filter for the state \underline{x}_k based on the previously discussed models is introduced. Particular implementations based on RHMs are presented in the next two sections.

We denote the probability density for the parameter vector \underline{x}_k after the incorporation of all measurements up to time step $k-1$ plus the measurements $\hat{\underline{y}}_{k,1}, \dots, \hat{\underline{y}}_{k,l}$ with $f_l(\underline{x}_k)$ for $0 \leq l \leq n_k$. In this article we focus on Gaussian

state estimators so that all probability densities are approximated with Gaussians, i.e., $f_l(\underline{x}_k) \approx \mathcal{N}(\underline{x}_k - \underline{\mu}_{x,l}^x, \underline{\Sigma}_{k,l}^x)$, where $\underline{\mu}_{x,l}^x$ is the mean and $\underline{\Sigma}_{k,l}^x$ the covariance matrix.

Time Update: The time update step predicts $f_{n_{k-1}}(\underline{x}_{k-1})$ to the next time step, i.e., it determines $f_0(\underline{x}_k)$. As we focus on linear system models (2), the time update can be performed with the Kalman filter formulas; see for example [1].

Measurement Update: The prediction $f_0(\underline{x}_k)$ is updated with the set of measurements $\{\hat{y}_{k,l}\}_{l=1}^{n_k}$ according to Bayes' rule. Because the measurement generation process is assumed to be independent for consecutive measurements, they can be incorporated recursively according to

$$f_l(\underline{x}_k) = \alpha_{k,l} \cdot f(\hat{y}_{k,l} | \underline{x}_k) \cdot f_{l-1}(\underline{x}_k) \text{ for } 1 \leq l \leq n_k$$

where $f(\hat{y}_{k,l} | \underline{x}_k)$ is a single measurement likelihood function and $\alpha_{k,l}$ is a normalization factor.

Note that the order of the measurements for a particular time step is irrelevant, because they are generated independently. However, the processing order may matter if approximations are performed (see remark 3).

V. ELLIPTIC SHAPES

Elliptic shape approximations are highly relevant for real world applications as many targets are approximately elliptic. Even in case of high measurement noise and few available measurements, an elliptic shape approximation can be estimated. In this section an implicit measurement equation is derived for elliptic shapes based on an RHM and subsequently a Gaussian state estimator is developed.

A. Parameterization of an Ellipse

An ellipse is determined by its center $\underline{m}_k \in \mathcal{R}^2$ and a positive semidefinite shape matrix $\mathbf{A}_k \in \mathcal{R}^{2 \times 2}$. Based on the Cholesky decomposition $(\mathbf{A}_k)^{-1} = \mathbf{L}_k \mathbf{L}_k^T$, where

$$\mathbf{L}_k := \begin{bmatrix} a_k & 0 \\ c_k & b_k \end{bmatrix} \quad (7)$$

a suitable vectorized parameterization $\underline{p}_k^{\text{el}} := [a_k, b_k, c_k]^T$ of \mathbf{A}_k can be defined. With $\underline{x}_k^{\text{el}} := [\underline{m}_k^T, (\underline{x}_k^*)^T, (\underline{p}_k^{\text{el}})^T]^T$, the implicit shape function becomes

$$g^{\text{el}}(\underline{z}_{k,l}, \underline{x}_k^{\text{el}}) := (\underline{z}_{k,l} - \underline{m}_k)^T \cdot \mathbf{A}_k^{-1} \cdot (\underline{z}_{k,l} - \underline{m}_k) - 1.$$

B. Implicit Measurement Equation

Thanks to the chosen representation of an ellipse, the implicit function for the scaled version of $\bar{S}(\underline{p}_k^{\text{el}})$ with scaling factor $s_{k,l}$ turns out to be

$$\tilde{g}^{\text{el}}(\underline{z}_{k,l}, \underline{x}_k^{\text{el}}, s_{k,l}) := (\underline{z}_{k,l} - \underline{m}_k)^T \cdot \mathbf{A}_k^{-1} \cdot (\underline{z}_{k,l} - \underline{m}_k) - s_{k,l}^2. \quad (8)$$

Equations (8) and (1) specify together an implicit measurement equation, which in this case coincides with

the problem of fitting an ellipse to noisy data points plus the additional random scaling factor.

C. Gaussian State Estimator

Approaches based on the Kalman filter for state estimation with implicit measurement equations such as (8) and (1) are well known in literature. Typically, the implicit measurement equation is linearized around the measurement and state in order to render it explicit; see for example [33]. Here, we propose to perform algebraic reformulations followed by a statistical linearization around the measurement source as described in the following. When (8) would be linear, we could rewrite the problem directly as an explicit measurement equation by plugging (1) into (8). As (8) is nonlinear an exact reformulation is not possible. Nevertheless this reformulation can be performed approximately. For this purpose the first step is to plug (1) into (8), i.e.,

$$\tilde{g}^{\text{el}}(\hat{y}_{k,l}, \underline{x}_k^{\text{el}}, s_{k,l}) = \tilde{g}(\underline{z}_{k,l} + \underline{v}_{k,l}, \underline{x}_{k,l}^{\text{el}}, s_{k,l}). \quad (9)$$

After some minor simplifications of (9) and exploiting (8), the following measurement equation

$$h^{\text{el}}(\underline{x}_k^{\text{el}}, \underline{v}_{k,l}, \underline{s}_{k,l}, \hat{y}_{k,l}) = 0 \quad (10)$$

with a pseudomeasurement 0 is obtained, where

$$h^{\text{el}}(\underline{x}_k^{\text{el}}, \underline{v}_{k,l}, \underline{s}_{k,l}, \hat{y}_{k,l}) := \tilde{g}^{\text{el}}(\hat{y}_{k,l}, \underline{x}_k^{\text{el}}, s_{k,l}) - 2(\underline{z}_{k,l} - \underline{m}_k)^T \mathbf{A}_k^{-1} \underline{v}_{k,l} - \underline{v}_{k,l}^T \mathbf{A}_k^{-1} \underline{v}_{k,l} - s_{k,l}^2 \quad (11)$$

maps the state $\underline{x}_k^{\text{el}}$, the measurement noise $\underline{v}_{k,l}$, the scaling factor $s_{k,l}$, and the measurement $\hat{y}_{k,l}$ to the pseudomeasurement.

However, the unknown measurement source $\underline{z}_{k,l}$ still occurs in (10). The basic idea here is to substitute $\underline{z}_{k,l} - \underline{m}_k$ in (10) with a proper point estimate. The easiest way to obtain a point estimate for $\underline{z}_{k,l} - \underline{m}_k$ is to consider the ellipse specified by the mean of the previous estimate, i.e., $\underline{\mu}_{k,l-1}^p$ and use the point with the smallest distance from the conic to the measurement $\hat{y}_{k,l}$ as a point estimate for obtaining a point estimate for $\underline{z}_{k,l} - \underline{m}_k$.

The measurement equation (10) can directly be used within Gaussian state estimators such as the unscented Kalman filter (UKF) [34] or analytic moment calculation

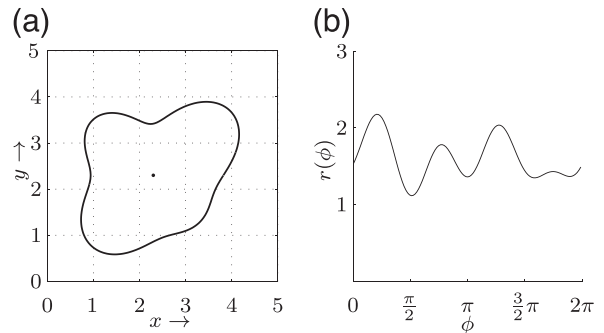


Fig. 4. Representation of star-convex shape with radius function. (a) Star-convex shape. (b) Radius function.

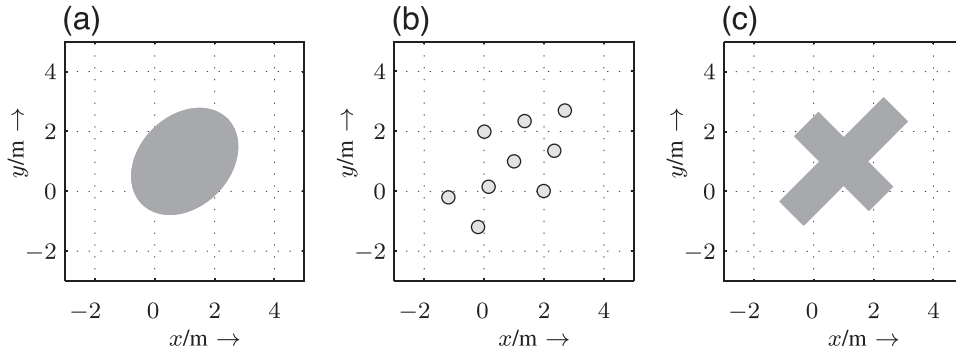


Fig. 5. Targets used for evaluation. (a) Target 1: Elliptic shape. (b) Target 2: Aircraft-like shape. (c) Target 3: Group target.

[35], which essentially performs a statistical linearization of (10). More precisely the joint density of the state and the predicted pseudomeasurement is approximated with a Gaussian. Then, the Kalman filtering [1] formulas can be used for calculating the updated estimate, i.e., given the previous estimate $f_{l-1}(\underline{x}_k) = N(\underline{x}_k - m_{k,l-1}^x, \Sigma_{k,l-1}^x)$, the updated estimate $f_l(\underline{x}_k) = N(\underline{x}_k - \mu_{k,l}^x, \Sigma_{k,l}^x)$ with the measurement $\hat{y}_{k,l}$ results from the Kalman filter⁵

$$\mu_{k,l}^x = \mu_{k,l-1}^x + \Sigma_k^{xh} \left(\Sigma_k^{hh} \right)^{-1} (0 - \mu_k^h) \quad (12)$$

$$\Sigma_{k,l}^x = \Sigma_{k,l-1}^x - \Sigma_k^{xh} \left(\Sigma_k^{hh} \right)^{-1} \Sigma_k^{hx} \quad (13)$$

where 0 is the predicted pseudomeasurement, Σ_k^{xh} is the covariance between the pseudomeasurement and the state, and Σ_k^{hh} is the variance of the predicted pseudomeasurement. In this manner a statistical linearization around the measurement source is performed. At this point it is important to note that μ_k^h and Σ_k^{xh} do not depend on the unknown measurement source $z_{k,l}$ and, hence, the error made due to substituting it with a point estimate is rather negligible.

REMARK 3 Due to the nonlinear measurement model and the performed approximations, the order of the measurement processing matters. However, we observed that the differences arising from different processing orders is rather negligible. Besides, it is possible to perform a batch processing of all measurements by means of stacking the single measurement functions (10). By this means, the estimation accuracy can be slightly increased.

REMARK 4 Due to the statistical linearization of the implicit measurement equation, approximation errors are introduced. As a consequence the resulting estimation quality depends highly on the parameterization of the ellipse and of the particular form of $\tilde{g}^{\text{el}}(\hat{y}_{k,l}, \underline{x}_k^{\text{el}}, s_{k,l})$. For

⁵For sake of clarity, the index “el” is omitted for the mean and covariance matrices of the estimates.

example, we observed that multiplying both sides of (9) with $1/\text{tr}(\mathbf{L}_k \mathbf{L}_k^T)$ improves the estimation quality.

REMARK 5 Note that the actual likelihood function $f(\hat{y}_{k,l} | x_k^{\text{el}})$ can be derived from the measurement equation (17), however, it is not required explicitly when performing statistical linearization.

VI. STAR-CONVEX SHAPES

When the measurement noise is low compared with the target extent, it may be possible to extract more detailed shape information than an ellipse from the measurements. For this purpose an RHM for estimating and tracking the parameters of a star-convex shape approximation is presented in the following. A detailed target shape approximation is of high value for many higher level problems such as target classification, track management, and sensor management. Last but not least a more detailed shape estimate results in a better estimation quality for the kinematic state of the target as it is a more precise model of the reality.

A. Parametrization of Star-Convex Shapes

A star-convex shape $S(\underline{p}_k^{\text{sc}})$ can be represented in parametric form with the help of a radius function $r(\underline{p}_k^{\text{sc}}, \phi)$, which gives the distance from the object center to a contour point depending on the angle ϕ and a parameter vector $\underline{p}_k^{\text{sc}}$ (see Fig 4). A suitable (finite-dimensional) parameterization $\underline{p}_k^{\text{sc}}$ of a radius function is given by the first N_f Fourier coefficients that define a Fourier series expansion [36, 37], i.e.,

$$\begin{aligned} r(\underline{p}_k^{\text{sc}}, \phi) &= \frac{1}{2} a_k^{(0)} + \sum_{j=1 \dots N_f} (a_k^{(j)} \cos(j\phi) + b_k^{(j)} \sin(j\phi)) \\ &= \mathbf{R}(\phi) \cdot \underline{p}_k^{\text{sc}} \end{aligned}$$

where

$$\begin{aligned} \mathbf{R}(\phi) &= [\frac{1}{2}, \cos(\phi), \sin(\phi), \dots, \cos(N_f \phi), \sin(N_f \phi)], \\ \text{and } \underline{p}_k^{\text{sc}} &= [a_k^{(0)}, a_k^{(1)}, b_k^{(1)}, \dots, a_k^{(N_f)}, b_k^{(N_f)}]^T. \end{aligned}$$

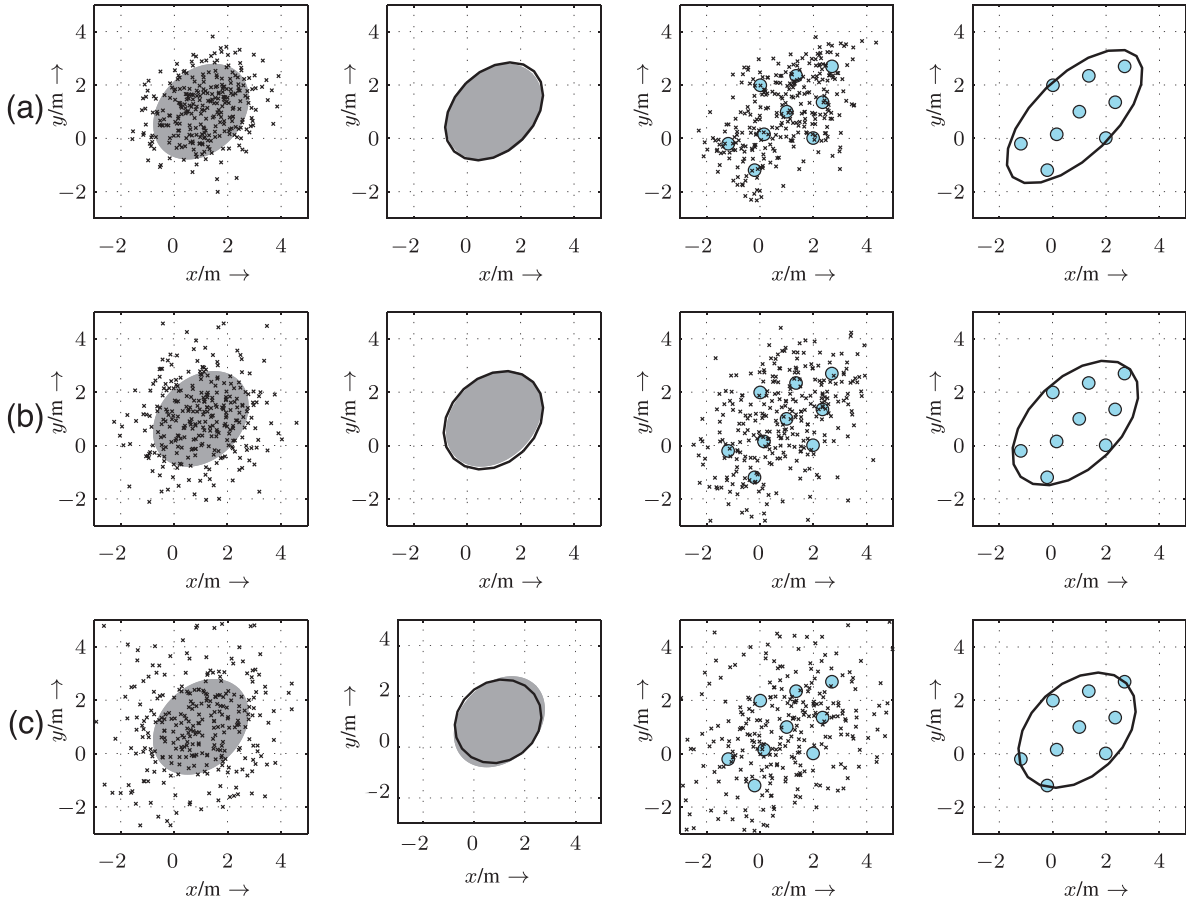


Fig. 6. Simulation results. Example measurements for particular run and point estimates for shape averaged over 20 runs. Simulations are performed with (a) low measurement noise level $\Sigma_{k,1}^v = \text{diag}(0.6^2, 0.6^2)$, (b) medium noise level $\Sigma_{k,1}^v = \text{diag}(1, 1)$, and (c) high measurement noise level $\Sigma_{k,1}^v = \text{diag}(1.4^2, 1.4^2)$.

Fourier coefficients with small indices encode information about the coarse features of the shape and Fourier coefficients with larger indices encode finer details.

B. Implicit Measurement Equation

With $\underline{x}_k^{\text{sc}} := [\underline{m}_k^T, (\underline{x}_k^*)^T, (\underline{p}_k^{\text{sc}})^T]^T$ and the implicit representation of star-convex curves [36], we obtain

$$g^{\text{sc}}(\underline{z}_{k,l}, \underline{x}_k^{\text{sc}}) = \|\underline{m} - \underline{z}_{k,l}\|^2 - r(\underline{p}_k^{\text{sc}}, \angle(\underline{m} - \underline{z}_{k,l}))^2 \quad (14)$$

where $\angle(\underline{m} - \underline{z}_{k,l})$ denotes the angle between $\underline{m} - \underline{z}_{k,l}$ and the x -axis. The scaled version of the shape boundary is specified by

$$\tilde{g}^{\text{sc}}(\underline{z}_{k,l}, \underline{x}_k^{\text{sc}}, s_{k,l}) = \|\underline{m} - \underline{z}_{k,l}\|^2 - s^2 \cdot r(\underline{p}_k^{\text{sc}}, \angle(\underline{m} - \underline{z}_{k,l}))^2 \quad (15)$$

Again, (15) specifies together with (1) an implicit measurement equation.

C. Bayesian State Estimator

A measurement equation can be derived by plugging (1) into (15)

$$\tilde{g}^{\text{sc}}(\hat{\underline{y}}_{k,l}, \underline{x}_k^{\text{sc}}, s_{k,l}) = \tilde{g}(\underline{z}_{k,l} + \underline{v}_{k,l}, \underline{p}_k^{\text{sc}}, s_{k,l}). \quad (16)$$

In order to avoid the treatment of uncertain angles, we propose to replace the angles in occurrences $r(\underline{p}_k^{\text{sc}}, \cdot)$ with a point estimate $\hat{\phi}_{k,l}$, i.e., we assume $r(\underline{p}_k^{\text{sc}}, \angle(\underline{m} - \hat{\underline{y}}_{k,l})) \approx r(\underline{p}_k^{\text{sc}}, \angle(\underline{m} - (\underline{z}_{k,l} + \underline{v}_{k,l}))) \approx r(\underline{p}_k^{\text{sc}}, \hat{\phi}_{k,l})$.

REMARK 6 A proper point estimate is given by the most likely angle $\phi_{k,l}$. In case of isotropic measurement noise, this point estimate $\phi_{k,l}$ is given by the angle between the vector from the current shape center estimate $\underline{\mu}_{k,l-1}^m$ to the measurement $\hat{\underline{y}}_{k,l}$ and the x -axis, i.e., $\hat{\phi}_{k,l} := \angle(\hat{\underline{y}}_{k,l} - \underline{\mu}_{k,l-1}^m)$.

Based on the point estimate and $\underline{m}_k - \underline{z}_{k,l} \approx s_{k,l} \cdot \mathbf{R}(\hat{\phi}_{k,l}) \cdot \underline{p}_k^{\text{sc}} \cdot \underline{e}(\hat{\phi}_{k,l})$, where $\underline{e}(\hat{\phi}_{k,l}) := [\cos \hat{\phi}_{k,l}, \sin \hat{\phi}_{k,l}]^T$, (16) can be simplified to the following measurement equation

$$h^{\text{sc}}(\underline{x}_k, \underline{v}_{k,l}, s_{k,l}, \hat{\underline{y}}_{k,l}) = 0 \quad (17)$$

with

$$h^{\text{sc}}(\underline{x}_k^{\text{sc}}, s_{k,l}, \hat{\underline{y}}_{k,l}) := s_{k,l}^2 \cdot \|\mathbf{R}(\hat{\phi}_{k,l}) \cdot \underline{p}_k^{\text{sc}}\|^2 + 2s_{k,l} \mathbf{R}(\hat{\phi}_{k,l}) \underline{p}_k^{\text{sc}} \underline{e}(\hat{\phi}_{k,l})^T \underline{v}_{k,l} + \|\underline{v}_{k,l}\|^2 - \|\hat{\underline{y}}_{k,l} - \underline{m}_k\|^2$$

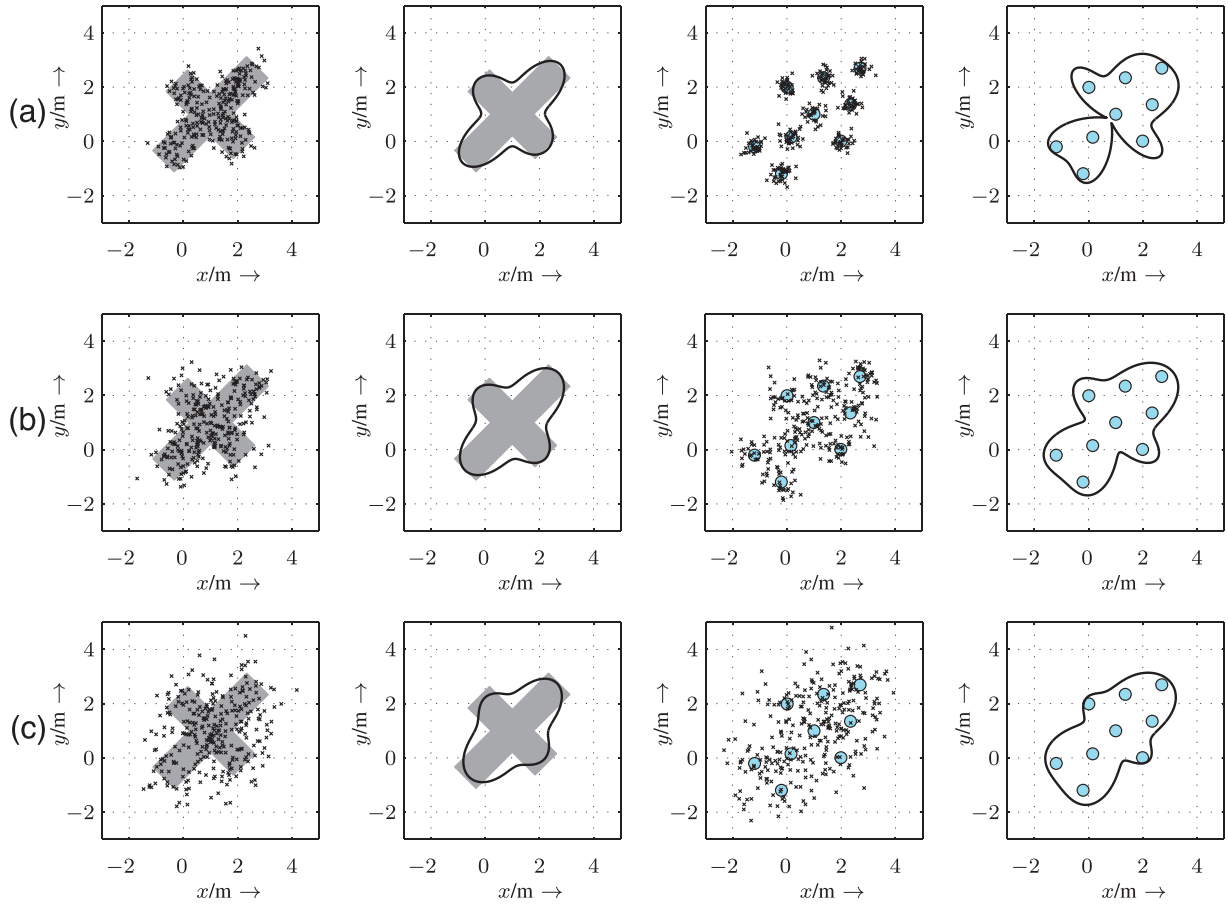


Fig. 7. Simulation results. Example measurements for particular run and point estimates for shape averaged over 20 runs. Simulations are performed with low (a) measurement noise level $\Sigma_{k,1}^v = \text{diag}(0.3^2, 0.3^2)$, (b) medium measurement noise level $\Sigma_{k,1}^v = \text{diag}(0.4^2, 0.4^2)$, and (c) high measurement noise level $\Sigma_{k,1}^v = \text{diag}(0.6^2, 0.6^2)$.

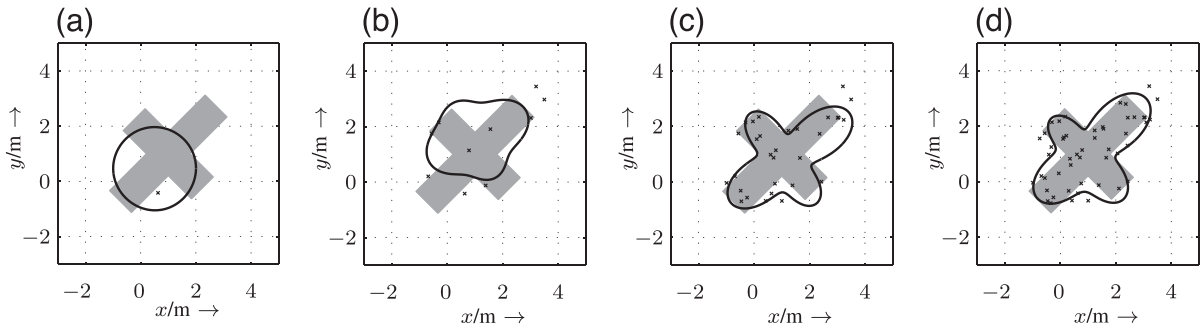


Fig. 8. Example run demonstrating sequential incorporation of measurements (noise level: $\Sigma_{k,1}^v = \text{diag}(0.3^2, 0.3^2)$). (a) First measurement. (b) 10 measurements. (c) 30 measurements. (d) 50 measurements.

which maps the state $\underline{x}_k^{\text{sc}}$, the measurement noise $\underline{v}_{k,l}$, the scaling factor $s_{k,l}$, and the measurement $\hat{y}_{k,l}$ to a pseudomeasurement 0.

REMARK 7 An alternative derivation of (17) based on the explicit representation of the shape with the radius function can be found in [35].

For a given density $f_{l-1}(\underline{x}_k) = N(\underline{x}_k - \underline{\mu}_{k,l-1}^x, \Sigma_{k,l-1}^x)$, the posterior density $f_l(\underline{x}_k) = \{N(\underline{x}_k - \underline{\mu}_{k,l}^x, \Sigma_{k,l}^x)\}$ having received the measurement $\hat{y}_{k,l}$ can be calculated with a Gaussian state estimator such as the UKF [34] or analytic moment calculation [35] for a closed-form measurement update. See also (12) and (13) in this

context. Just as for ellipses the order of the measurement processing matters (see the discussion in remark 3).

VII. EVALUATION

RHMs for elliptic and star-convex shapes are evaluated by means of both stationary and moving extended objects.⁶ For both elliptic shapes and star-convex shapes the UKF [34] is used for performing the measurement update. For elliptic shapes the squared scaling factor is modeled as a Gaussian distribution with mean 0.5 and variance 1/12 (i.e., the first two moments of a uniform distribution). For star-convex shapes the scaling factor is modeled as Gaussian distribution with mean 0.7 and variance 0.06.

A. Stationary Extended Target

In the first scenario we consider an extended object with fixed position and shape. From the target 300 measurements are received sequentially, i.e., a single measurement per time step ($n_k = 1$). Simulations are performed with the three different target types depicted in Fig. 5, where measurement sources are drawn uniformly from the target surface/group members.

The parameters of the ellipse are a priori set to a Gaussian with mean $[0.5, 0.5, 1.6, 1.6, 0.6]^T$ and covariance matrix $\text{diag}(3, 3, 0.5, 0.5, 0.5)$, i.e., an uncertain circle with radius 1.2 and center $[0.5, 0.5]^T$. For the star-convex shape approximation, 15 Fourier coefficients are used, where the shape parameters are a priori set to a Gaussian with mean $[0.5, 0.5, 3, 0, \dots, 0]^T$ and covariance matrix $\text{diag}(0.7, 0.7, 0.1, 0.1, \dots, 0.1)$, i.e., an uncertain circle with radius 1.5 and center $[0.5, 0.5]^T$.

The estimation results after the 300 measurements are depicted in Fig. 6 and Fig. 7 for different measurement noise levels.

The shape estimates are averaged over 20 Monte-Carlo runs. In order to illustrate the magnitude of the measurement noise, the measurements of a particular run are also plotted. It is important to note that this is just done for visualization as the estimator incorporates the measurements recursively. Fig. 8 depicts a single example run for star-convex shapes in order to show the evolution of the shape estimates with an increasing number of measurements.

B. Moving Extended Object

In the second scenario the aircraft-shaped target shown in Fig. 9(a) moves along the trajectory depicted in Fig. 9(b). The measurement sources are drawn uniformly from the target surface. The magnitude of the measurement noise varies from measurement to measurement in order to simulate different sensors or different target-to-sensor geometries. The covariance matrix of the measurement noise is

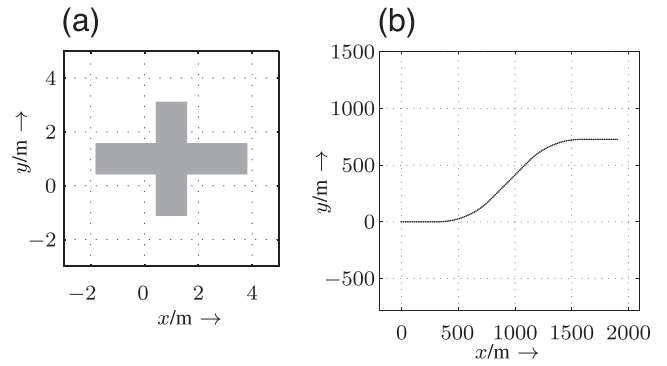


Fig. 9. Extended object and its trajectory. (a) Target shape. (b) Trajectory of the target.

$\sum_{k,1}^v = \text{diag}(0.2^2, 0.2^2)$ with probability 0.75 and $\sum_{k,1}^v = \text{diag}(0.4^2, 0.4^2)$ with probability 0.25. The number of measurements received per time instant is given by $n_k = n_k^* + 1$, where n_k^* is a Poisson distributed random variable with mean 4 for the ellipse and mean 7 for the star-convex shape.

We employ a constant velocity model for the temporal evolution of the target center [1] and a random walk model for the shape parameters. Hence, the state vector to be tracked is $\underline{x}_k = \left[\underline{m}_k, \underline{m}_k^v, \left(\underline{p}_k^{\text{sc}} \right)^T \right]^T$ where \underline{m}_k is the center, \underline{m}_k^v is the velocity vector, and $\underline{p}_k^{\text{sc}}$ are the shape parameters. As the center is assumed to evolve according to a constant velocity model, the system matrix in (2) is $\mathbf{A}_k = \text{diag}(\mathbf{A}_k^{cv}, \mathbf{I}_d)$, where $\mathbf{A}_k^{cv} = \begin{bmatrix} \mathbf{I}_2 & T\mathbf{I}_2 \\ 0 & \mathbf{I}_2 \end{bmatrix}$ with $T = 1$ and \mathbf{I}_d is the identity matrix with dimension $d = 5$ for ellipses and $d = 11$ for star-convex shapes. The system noise is zero-mean Gaussian noise with covariance matrix $\mathbf{C}_k^w = \text{diag}(q_1 \cdot \mathbf{I}_d, \mathbf{C}_k^{cv})$ with $\mathbf{C}_k^{cv} = q_2 \begin{bmatrix} \frac{T^3}{3}\mathbf{I}_2 & \frac{T^2}{2}\mathbf{I}_2 \\ \frac{T^2}{2}\mathbf{I}_2 & T\mathbf{I}_2 \end{bmatrix}$. For the ellipse we have $q_1 = 0.0015$ and $q_2 = 0.005$. For the star-convex shape $q_1 = 0.0001$ and $q_2 = 0.003$.

The estimated shapes (averaged over 20 time steps) are depicted in Fig. 10 and Fig. 11 for two snippets of the trajectory. The results show that the shape of the extended object is tracked precisely, even when the shape changes its orientation.

Note that in the simulations with elliptic shapes the number of measurements per time step is lower than for star-convex shapes. A star-convex shape approximation can only be extracted well in case the measurements carry enough information, i.e., enough measurements with rather low noise are available.

The example measurements in Fig. 10 and Fig. 11 also emphasize that naïve approaches for estimating a shape would be bound to fail, e.g., directly computing an enclosing shape of the measurements is infeasible because the measurements are noisy and only a couple of measurements are available per time step.

⁶Source code for RHMs is available at <http://www.cloudrunner.eu>.

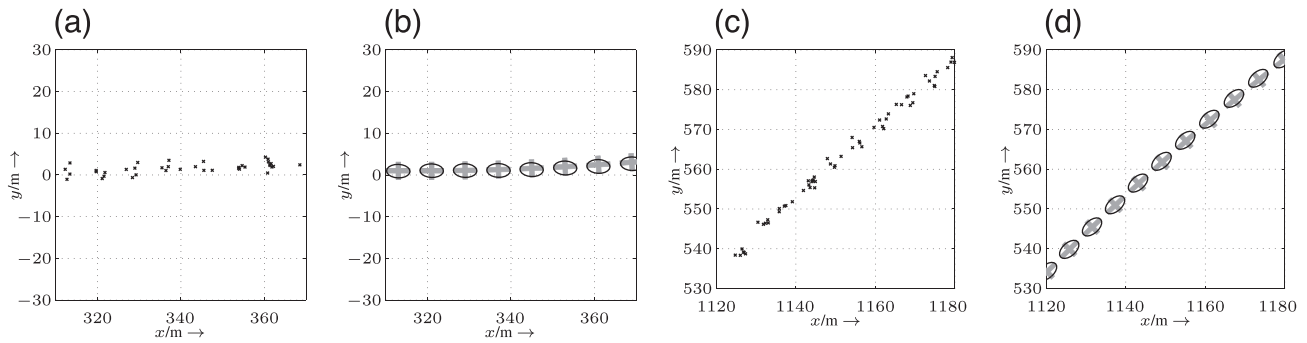


Fig. 10. Tracking extended object with RHM for ellipses: example measurements from particular run and average shape estimates. (a) Example measurements. (b) Shape estimates. (c) Example measurements. (d) Shape estimates.

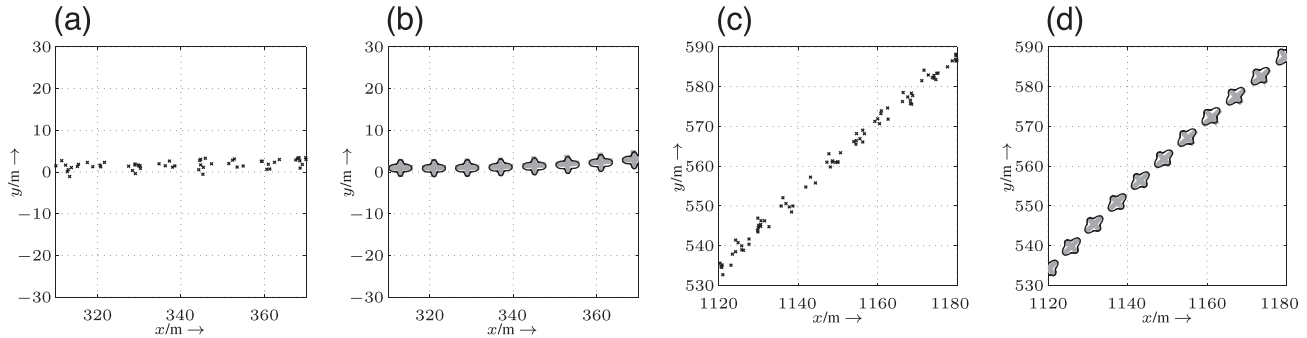


Fig. 11. Tracking extended object with RHM for star-convex shapes: example measurements from particular run and average shape estimates. (a) Example measurements. (b) Shape estimates. (c) Example measurements. (d) Shape estimates.

VIII. CONCLUSIONS AND FUTURE WORK

This article considered the problem of estimating a shape approximation of an extended object, which gives rise to several measurements from different spatially distributed measurement sources. For this purpose a novel approach for modeling extended objects called RHM was introduced that allows to derive a functional relationship between the measurements and shape parameters. We presented particular RHMs for elliptic and free-form star-convex shapes and derived measurement equations for which standard Gaussian state estimators can be used. Nevertheless, estimating a detailed star-convex shape approximation is only possible when the measurement noise is rather low compared with target extent and enough measurements per time step are available. If this is not the case, a basic shape such as an ellipse is more suitable. Hence, a mechanism for adapting the complexity of the used shape description is desired. The capability of estimating free-form shape approximations paves the way for new applications, e.g., classification based on the shape and group splitting detection.

REFERENCES

- [1] Bar-Shalom, Y., Kirubarajan, T., and Li, X.-R. *Estimation with Applications to Tracking and Navigation*. Hoboken, NJ: Wiley, 2002.
- [2] Gilholm, K. and Salmond, D. Spatial distribution model for tracking extended objects. *IEE Proceedings – Radar, Sonar and Navigation*, **152**, 5 (Oct. 2005), 364–371.
- [3] Koch, J. W. Bayesian approach to extended object and cluster tracking using random matrices. *IEEE Transactions on Aerospace and Electronic Systems*, **44**, 3 (July 2008), 1042–1059.
- [4] Baum, M., Noack, B., and Hanebeck, U. D. Extended object and group tracking with elliptic random hypersurface models. In *Proceedings of the 13th International Conference on Information Fusion (Fusion 2010)*, Edinburgh, UK, July 2010.
- [5] Gilholm, K. et al. Poisson models for extended target and group tracking. In *Proceedings of SPIE*, vol. 5913, *Signal and Data Processing of Small Targets*, 2005.
- [6] Boers, Y. et al. Track-before-detect algorithm for tracking extended targets. *IEE Proceedings – Radar, Sonar and Navigation*, **153**, 4 (Aug. 2006), 345–351.
- [7] Angelova, D. and Mihaylova, L. Extended object tracking using Monte Carlo methods. *IEEE Transactions on Signal Processing*, **56**, 2 (Feb. 2008), 825–832.
- [8] Petrov, N. et al. A novel sequential Monte Carlo approach for extended object tracking based on border parameterization. In *Proceedings of the 14th International Conference on Information Fusion (Fusion 2011)*, Chicago, IL, July 2011.
- [9] Petrov, N. et al. Box particle filtering for extended object tracking. In *15th International Conference on Information Fusion (Fusion 2012)*, July 2012, pp. 82–89.

- [10] Petrov, N. et al.
Group object tracking with a sequential Monte Carlo method based on a parameterised likelihood function.
In Monte Carlo Methods and Applications: Proceedings of the 8th IMACS Seminar on Monte Carlo Methods. Berlin: De Gruyter, 2012, pp. 171–180.
- [11] Feldmann, M., Fränken, D., and Koch, W.
Tracking of extended objects and group targets using random matrices.
IEEE Transactions on Signal Processing, **59**, 4 (2011), 1409–1420.
- [12] Degerman, J., Wintenby, J., and Svensson, D.
Extended target tracking using principal components.
In Proceedings of the 14th International Conference on Information Fusion (Fusion 2011), Chicago, IL, July 2011.
- [13] Lan, J. and Rong Li, X.
Tracking of extended object or target group using random matrix - Part I: New model and approach.
In 15th International Conference on Information Fusion (Fusion 2012), July 2012, pp. 2177–2184.
- [14] ———.
Tracking of extended object or target group using random matrix - Part II: Irregular object.
In 15th International Conference on Information Fusion (Fusion 2012), July 2012, pp. 2185–2192.
- [15] Wieneke, M. and Koch, W.
A PMHT approach for extended objects and object groups.
IEEE Transactions on Aerospace and Electronic Systems, **48**, 3 (July 2012), 2349–2370.
- [16] Mahler, R. P. S.
PHD filters for nonstandard targets, I: Extended targets.
In Proceedings of the 12th International Conference on Information Fusion (Fusion 2009), Seattle, WA, July 2009.
- [17] Granström, K., Lundquist, C., and Orguner, U.
A Gaussian mixture PHD filter for extended target tracking.
In Proceedings of the 13th International Conference on Information Fusion (Fusion 2010), Edinburgh, UK, July 2010.
- [18] Orguner, U., Granström, K., and Lundquist, C.
Extended target tracking with a cardinalized probability hypothesis density filter.
In Proceedings of the 14th International Conference on Information Fusion (Fusion 2011), Chicago, IL, July 2011.
- [19] Lundquist, C., Granström, K., and Orguner, U.
Estimating the shape of targets with a PHD filter.
In Proceedings of the International Conference on Information Fusion, Chicago, IL, July 2011.
- [20] Granström, K. and Orguner, U.
A PHD filter for tracking multiple extended targets using random matrices.
IEEE Transactions on Signal Processing, **60**, 11 (Nov. 2012), 5657–5671.
- [21] Baum, M. and Hanebeck, U. D.
Extended object tracking based on combined set-theoretic and stochastic fusion.
In Proceedings of the 12th International Conference on Information Fusion (Fusion 2009), Seattle, WA, July 2009.
- [22] ———.
Extended object tracking based on set-theoretic and stochastic fusion.
IEEE Transactions on Aerospace and Electronic Systems, **48**, 4 (Oct. 2012), 3103–3115.
- [23] Baum, M. et al.
Extended object and group tracking: A comparison of random matrices and random hypersurface models.
In Proceedings of the IEEE ISIF Workshop on Sensor Data Fusion: Trends, Solutions, Applications (SDF 2010), Leipzig, Germany, Oct. 2010.
- [24] Baum, M. and Hanebeck, U. D.
Shape tracking of extended objects and group targets with star-convex RHMs.
In Proceedings of the 14th International Conference on Information Fusion (Fusion 2011), Chicago, IL, July 2011.
- [25] ———.
Random hypersurface models for extended object tracking.
In Proceedings of the 9th IEEE International Symposium on Signal Processing and Information Technology (ISSPIT 2009), Ajman, United Arab Emirates, Dec. 2009.
- [26] Baum, M., Noack, B., and Hanebeck, U. D.
Random hypersurface mixture models for tracking multiple extended objects.
In Proceedings of the 50th IEEE Conference on Decision and Control (CDC 2011), Orlando, FL, Dec. 2011.
- [27] Baum, M., Klumpp, V., and Hanebeck, U. D.
A novel Bayesian method for fitting a circle to noisy points.
In Proceedings of the 13th International Conference on Information Fusion (Fusion 2010), Edinburgh, UK, July 2010.
- [28] Baum, M. and Hanebeck, U. D.
Fitting conics to noisy data using stochastic linearization.
In Proceedings of the 2011 IEEE/RSJ International Conference on Intelligent Robots and Systems (IROS 2011), San Francisco, CA, Sept. 2011.
- [29] Baum, M.
Student research highlight: Simultaneous tracking and shape estimation of extended targets.
IEEE Aerospace and Electronic Systems Magazine, **27**, 7 (July 2012), 42–44.
- [30] ———.
Simultaneous tracking and shape estimation of extended objects. Dissertation, Karlsruhe Institute of Technology (KIT), ISAS - Intelligent Sensor-Actuator-Systems Laboratory, 2013.
- [31] Faion, F., Baum, M., and Hanebeck, U. D.
Tracking 3D shapes in noisy point clouds with random hypersurface models.
In Proceedings of the 15th International Conference on Information Fusion (Fusion 2012), Singapore, July 2012.
- [32] Chernov, N.
Circular and Linear Regression: Fitting Circles and Lines by Least Squares. Boca Raton, FL: CRC Press, 2010.
- [33] Soatto, S., Frezza, R., and Perona, P.
Motion estimation via dynamic vision.
IEEE Transactions on Automatic Control **41**, 3 (1996), 393–413.
- [34] Julier, S. J. and Uhlmann, J. K.
Unscented filtering and nonlinear estimation.
Proceedings of the IEEE, **92**, 3 (2004), 401–422.
- [35] Baum, M. et al.
Optimal Gaussian filtering for polynomial systems applied to association-free multi-target tracking.
In Proceedings of the 14th International Conference on Information Fusion (Fusion 2011), Chicago, IL, July 2011.
- [36] Ünsalan, C. and Ercil, A.
Conversions between parametric and implicit forms using polar/spherical coordinate representations.
Computer Vision and Image Understanding, **81**, 1 (2001), 1–25.
- [37] Zhang, D. and Lu, G.
Study and evaluation of different Fourier methods for image retrieval.
Image and Vision Computing, **23**, 1 (2005), 33–49.



Marcus Baum received the Dipl.-Inform. degree in computer science from the University of Karlsruhe (TH), Germany, in 2007. Currently, he is working towards a PhD degree at the Intelligent Sensor-Actuator-Systems Laboratory, Karlsruhe Institute of Technology (KIT), Germany. His research interests are in the field of extended object tracking, multi-target tracking, nonlinear estimation, and sensor data fusion.

From October to December 2011, he was a visiting researcher with Peter Willett at the University of Connecticut. Since 2010, he has been organizing the special session Extended Object and Group Tracking at the International Conference on Information Fusion (FUSION) together with Uwe D. Hanebeck and Wolfgang Koch.

Mr. Baum received the Best Student Paper Award of the 14th International Conference on Information Fusion (Fusion 2011), Chicago, IL for the paper “Shape Tracking of Extended Objects and Group Targets with Star-Convex RHM’s” (together with Uwe D. Hanebeck).

Uwe D. Hanebeck obtained his Ph.D. degree in 1997 and his habilitation degree in 2003, both in electrical engineering from the Technical University in Munich, Germany.

He is a chaired professor of Computer Science at the Karlsruhe Institute of Technology (KIT) in Germany and director of the Intelligent Sensor-Actuator-Systems Laboratory (ISAS). Since 2005, he is the chairman of the Research Training Group RTG 1194 Self-Organizing Sensor-Actuator-Networks financed by the German Research Foundation. His research interests are in the areas of information fusion, nonlinear state estimation, stochastic modeling, system identification, and control with a strong emphasis on theory-driven approaches based on stochastic system theory and uncertainty models. Research results are applied to various application topics such as localization and tracking, human-robot-interaction, assistive systems, sensor-actuator-networks, medical engineering, distributed measuring system, and extended range telepresence. Research is pursued in many academic projects and in a variety of cooperations with industrial partners.



Dr. Hanebeck was the General Chair of the 2006 IEEE International Conference on Multisensor Fusion and Integration for Intelligent Systems (MFI 2006), Program Co-Chair of the 11th International Conference on Information Fusion (Fusion 2008), Program Co-Chair of the 2008 IEEE International Conference on Multisensor Fusion and Integration for Intelligent Systems (MFI 2008), Regional Program Co-Chair for Europe for the 2010 IEEE/RSJ International Conference on Intelligent Robots and Systems (IROS 2010), and Technical Co-Chair for the 16th International Conference on Information Fusion (Fusion 2013). He is a Member of the Board of Directors of the International Society of Information Fusion (ISIF), Associate Editor-in-Chief of its *Journal of Advances in Information Fusion* (JAIF), and Associate Editor for letters of the *IEEE Transactions on Aerospace and Electronic Systems* (TAES). He is author and coauthor of more than 260 publications in various high-ranking journals and conferences.